Free Radical Biology and Medicine 134 (2019) 359–373

Contents lists available at ScienceDirect

Free Radical Biology and Medicine

journal homepage: www.elsevier.com/locate/freeradbiomed

Original article

Mitochondrial translocation of estrogen receptor β affords resistance to oxidative insult-induced apoptosis and contributes to the pathogenesis of endometriosis

Tien-Ling Liao[a,b,c], Yu-Ching Lee[d], Chii-Ruey Tzeng[e], Yi-Pei Wang[a,c], Heng-Yu Chang[f], Yung-Feng Lin[b,c], Shu-Huei Kao[b,c,e,*]

[a] Graduate Institute of Medical Science, College of Medicine, Taipei Medical University, Taipei, Taiwan
[b] Ph.D. Program in Medical Biotechnology, College of Medical Science and Technology, Taipei Medical University, Taipei, Taiwan
[c] School of Medical Laboratory Science and Biotechnology, College of Medical Science and Technology, Taipei Medical University, Taipei, Taiwan
[d] The Center of Translational Medicine, Taipei Medical University, Taipei, Taiwan
[e] Center for Reproductive Medicine and Sciences, Taipei Medical University Hospital, Taipei, Taiwan
[f] Department of Biochemistry and Molecular Cell Biology, College of Medicine, Taipei Medical University, Taipei, Taiwan

ARTICLE INFO

Keywords:
Endometriosis
Cell migration
Mitochondrial estrogen receptor β
Mitochondrial bioenergetics
Oxidative stress
Anti-apoptosis

ABSTRACT

Endometriosis is the major cause of female infertility and has been linked to the action of estrogen and estrogen receptor (ER). A new pool of ERβ locates within mitochondria, which regulates the endometriotic cell withstanding external insults, but its effect remains controversial. We hypothesize that mitochondrial estrogen receptor ERβ (mtERβ) is a pivotal regulator in estradiol-mediated cell protection leading to the endometriotic progression. We observed elevated levels of ERβ in the endometriotic tissues. A dramatic increase of ERβ in mitochondria (mtERβ) was found in the ectopic endometriotic tissues, or the estradiol-primed primary endometriotic cells. We analyzed the mtERβ-specific overexpressing clone (mtsERβ), which exhibited higher mitochondrial bioenergetics and lower reactive oxygen species (ROS) generation. The mtsERβ-overexpressed endometriotic cells displayed an enhanced migration phenotype, whereas significantly attenuated migration by mitochondrial respiratory inhibitor (oligomycin) or ERβ deficiency by shERβ. Further investigations revealed that ERβ directly modulated mitochondrial DNA (mtDNA) gene expression by interacting with mtDNA D-loop and polymerase γ. The mtsERβ afforded a resistance to oxidative insult-induced apoptosis through the induction of the ROS scavenger enzyme Mn-superoxide dismutase and anti-apoptotic protein Bcl-2. Collectively, the demonstration of mtERβ responses in restoration of mitochondrial bioenergetics and inhibition of mitochondria-dependent apoptotic events provides insight into the pathogenesis of endometriosis, suggesting ERβ-selective estrogen receptor modulator may serve as novel therapeutics of endometriosis in the future.

1. Introduction

Endometriosis, one of the most frequent diseases of gynecology, represents an extensive threat to the physical, psychological and social integrity of women with reproductive age. Endometriosis is characterized as a benign but chronic estrogen-related disorder that shares certain features with tumors, such as a propensity for invasion, unrestrained growth, and extensive spreading [1]. It has been investigated that endometriosis is associated with two types of ovarian cancers, clear cell carcinoma and endometrioid adenocarcinoma [2–5]. Hyperplasia or metaplasia is frequently found in the precancerous stage. The changes of cell phenotype in metaplasia are between epithelial and mesenchymal states, defined as the epithelial–mesenchymal transition (EMT) and mesenchymal–epithelial transition (MET), which are central to the metastasis of many carcinomas and endometriosis [6–8]. The proliferative, migratoratory, and invasive properties of endometriotic cells that contribute to the development of endometriosis depend, in part, on the excessive local production of estrogen from a positive-feedback loop of estrogen production [1,6]. In clinical treatment, estrogen overproduction can be suppressed by gonadotropin-releasing hormone agonist (GnRHa) therapy to reduce lesion sizes.

Evidence showed that elevated levels of estrogen receptor β (ERβ)

* Corresponding author. School of Medical Laboratory Science and Biotechnology, Ph.D. Program in Medical Biotechnology, Taipei Medical University, Taipei 110, Taiwan.
E-mail address: kaosh@tmu.edu.tw (S.-H. Kao).

https://doi.org/10.1016/j.freeradbiomed.2019.01.022
Received 20 October 2018; Received in revised form 10 January 2019; Accepted 20 January 2019
Available online 24 January 2019
0891-5849/

in endometriotic tissues [8–10], but declined in carcinogenesis [11]. However, the levels of estrogen receptor α (ERα) were notable lower in endometriotic tissues [12]. The mechanism responsible for estrogen-induced survival of ectopic endometriotic cells has been linked to ERβ-mediated signaling pathways [1,8,10,13]. An altered balance of ERβ subcellular distribution may initiate physiological and pathological process that leads to diseases [14]. Studies have shown that cytoplasmic ERβ interacts with apoptotic machinery and inflammasome complexes in the ectopic lesion to drive ectopic lesion survival [8]. Moreover, the distributional differences in cytoplasmic and nuclear ERβ have been observed in the clinical patients with endometriosis, endometrial cancer, advanced ovarian cancer, and non-small-cell lung cancer [14–16]. In addition to cytoplasmic and nuclear ERβ, it has been observed that ERβ translocated into mitochondria of various mammalian cells [15,17–19]. These observations prompted us to investigate whether the mitochondrial distribution of ERβ (mtERβ) might play a pivotal role in modulating the survival and metaplasia of endometriotic tissues.

Endometriosis has been recognized as high energy-demanded process for endometriotic cell movement and attachment to the ectopic lesion [20]. The excessive mitochondrial respiration and abnormal mitochondrial function leads to the enhanced generation of reactive oxygen species (ROS) contributing to the pathogenesis of clinical diseases and aging [21,22]. Similarly, the enhanced accumulation of mitochondrial DNA (mtDNA) mutations and oxidative damages were found in the endometriotic tissues [23,24]. In addition, estrogen at physiological level enhances oxidative phosphorylation activity and sustains mitochondrial energy-transducing capacity. Therefore, the mtERβ might be associated with energy-related pathways within the mitochondria. These mtERβ-mediated processes whether subsequently affect the cell apoptosis and progressive transformation of estrogen-related cancer remain unclear and need to be addressed.

This is the first demonstration to examine whether mtERβ is responsible for regulating mitochondrial bioenergetics, oxidative stress response pathway, and anti-apoptosis which contributes to participate in pathological development of endometriosis. We show an increase of ERβ in endometriosis, and the augmented ERβ promotes endometriotic cell migration. Establishment of a cell model for specific mitochondrial localization of ERβ serves as an excellent model for observing the direct effects of mtERβ with or without estrogen activation. This study characterizes mtERβ improved the mitochondrial function, and enhance the survival of endometriotic cells by preserving energetic usage and sanitizing ROS insults leading to the pathogenesis of endometriosis.

2. Materials and methods

2.1. Clinical specimens

One hundred fifty clinical samples of defined adenomyosis (n = 44), ovarian endometrioma (n = 47), myoma (n = 37), and non-lesion (n = 22) were obtained from surgical patients undergoing laparotomic hysterectomy at the Department of Gynecology and Obstetrics, Taipei Medical University Hospital. This study was performed according to the tenets of the Declaration of Helsinki for research involving human subjects. All specimens were collected under the protocol immediately after hysterectomy with approval of the Institutional Review Board of Taipei Medical University Hospital.

2.2. Reagents

Unless otherwise specified, chemicals were purchased from Sigma-Aldrich (Sigma, Tokyo, Japan), culture media and supplements were obtained from Invitrogen (Carlsbad, CA, USA). MitoTracker Red, 4′,6-diamidino-2-phenylindole (DAPI), 5,5′,6,6′-tetrachloro-1,1′,3,3′-tetraethylbenzimidazolo-carbocyanine iodide (JC-1), and MitoSOX™ Red were obtained from Thermo Fisher Scientific (MA, USA). ER ligand, 17β-Estradiol (E2); ER antagonist, ICI 182780; and ERβ agonist, diarylpropionitrile (DPN), were obtained from Tocris Bioscience (Bristol, UK). The anti-ERβ, anti-β-actin, anti-mitochondrial transcription factor A (TFAM) (Santa Cruz Biotechnology, St. Louis, MO, USA); anti-COX-IV (Abnova, Pforzheim, Germany); anti-VDAC, anti-Bcl-2, anti-cytochome *c* (BD Biosciences, NSW, Australia), anti-nuclear-derived nuclear respiratory factor 1 (NRF-1), and anti-caspase 3 (Cell Signaling Technology, Beverly, MA, USA) were purchased.

2.3. Cell culture and conditions

Human primary endometrial cells derived from clinical endometrial samples were isolate and cultured in phenol red-free Dulbecco's Modified Eagle's Medium/Nutrient F-12 Ham (DMEM/F12) medium supplemented with 10% charcoal/dextran-treated fetal bovine serum (FBS), 100 U/ml penicillin G sodium, and 100 μg/ml streptomycin sulfate, in a cell incubator (5% CO_2 at 37 °C). Cells were cultured in phenol red-free DMEM/F12 medium without FBS for 24 h before reagent treatments or transfection.

2.4. PCR, real-time quantitative PCR (qPCR), and long range PCR

Real-time qPCR amplification was performed with Roche LightCycler® System and LightCycler® FastStart DNA Masterplus SYBR Green I (Roche Applied Science, Basel, Switzerland) according the manufacturer's instructions. The primer sequences are listed below: ERβ (*ESR2*)-qF, 5′-CTCTTTGAACCTGGACCAGTA-3’; ERβ (*ESR2*)-qR, 5′-TTCCCAGCAATGTCACTAACT-3’; E-Cadherin-qF, 5′-CCCGGGACAA CGTTTATTAC-3’; E-Cadherin-qR, 5′-GCTGGCTCAAGTCAAAGTCC-3’; N-Cadherin-qF, 5′-CACTGCTCAGGACCCAGAT-3’; N-Cadherin-qR, 5′-TAAGCCGAGTGATGGTCC-3’; Vimentin-qF, 5′-GAGAACTTTGCCGTTG AAGC-3’; Vimentin-qR, 5′-TCCAGCAGCTTCCTGTAGGT-3’; NRF-1-qF, 5′-TTGGAGAATGTGGTGCGTAAGT-3’; NRF-1-qR, 5′-GAGAGGCGGCA GTTCTGAGT-3’; TFAM-qF, 5′-TTCCCTCCAACGCTGGGCAATT-3’; TFAM-qR, 5′-GTGGTTTTCATCTGTCTTGGCAAG-3’; manganese superoxide dismutase (MnSOD, *SOD2*)-qF, 5′-GGTAGCACCAGCACTAGCAG-3’; MnSOD (*SOD2*)-qR, 5′-CTGCAGTACTCTATACCACTACA-3’; β-actin-qF, 5′-CCAACCGCGAGAAGATGA-3’; β-actin-qR, 5′-CCAGAGGCGTACA GGGATAG-3’; L7901, 5′-TGAACCTACGAGTACACCGA-’3, and H16255, 5′-CTTTGGAGTTGCAGTTGATG-’3. Amplification efficiency for each tested genes were normalized to β-actin.

2.5. Scratch assay

A scratch assay was used to measure migratory rates. Cells were seeded with mitomycin C to inhibit proliferation and allow attaching, spreading, and forming a confluent monolayer. A culture-insert was used to generate a discrete area of the confluent monolayer to form a cell-free zone into which cells at the edges of the wound can migrate. Chemicals as 10 nM DPN or 1 μM oligomycin was added to the wells and images of cell movement were captured at regular intervals within a 48-h period for data analysis. The percentages of migratory area were calculated in indicated cell treated with DPN, oligomycin and transfected with ERβ-shRNA.

2.6. Determination of lipid peroxides by high-performance liquid chromatography (HPLC)

The content of lipid peroxide was determined in the form of malondialdehyde (MDA) as thiobarbituric acid reactive substance (TBARS). An aliquot of tissue lysates was mixed with 0.6 ml of 0.44 M phosphoric acid and 0.2 ml of a 42 mM thiobarbituric acid solution then proceeded at 95 °C for 1 h. The samples were then neutralized with 1 N NaOH in methanol before the HPLC analysis using a C_{18} column (4.6 × 250 mm, with a particle size of 5 μm, 200 × 4.6 mm, JT Baker, Phillipsburg, NJ) on an HPLC system (Jasco, Easton, MD, USA) with a solvent system composed of methanol and 50 mM phosphate buffer (pH 6.8) (4:6, v/v)

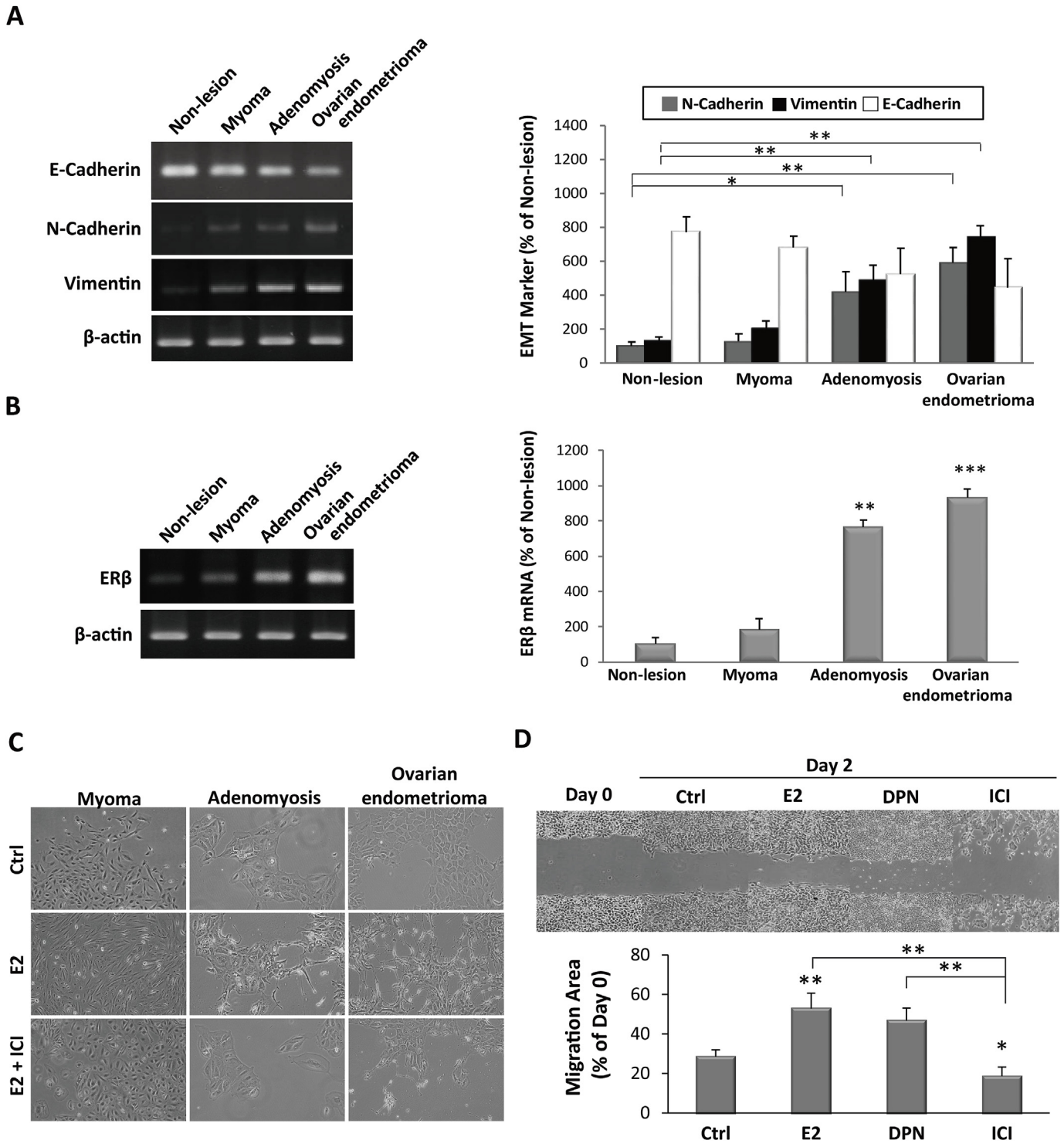

Fig. 1. High levels of *ERβ* mRNA with mesenchymal-like phenotypic changes were found in the endometriotic tissues. (A) The electrophoretograms and quantification for the mRNA levels of *E-cadherin, N-cadherin* and *vimentin* in the non-lesion, myoma, adenomyosis, and ovarian endometrioma were performed by PCR and real-time quantitative PCR (qPCR), respectively. The relative change of *N-cadherin*, *E-cadherin* and *vimentin* in different group was compared to the *N-cadherin* expression level of non-lesion group. (B) The electrophoretograms and quantification for the mRNA levels of *ERβ* were shown. Enhanced expression of mesenchymal markers (*N-cadherin* and *vimentin*) and *ERβ* were found in the endometriotic tissues. (C) Phase-contrast images of the cells established from myoma, adenomyosis, and ovarian endometrioma were presented. The endometriotic cells were variably treated with 10 nM estradiol (E2) or E2 with ER antagonist, ICI 182780 (ICI). The morphology changes from epithelial-like to a mesenchymal-like phenotype in the endometriotic cells were compared with control cells. (D) Endometriotic cell migration was assessed by the scratch assay. The percentages of wound area were normalized with the area at 0 h, and vary with the treatments. ER antagonist, ICI 182780 (ICI), blocked the estradiol-induced endometriotic cell migration. ER ligand, 17β-Estradiol (E2); ER antagonist, ICI 182780; and ERβ agonist, diarylpropionitrile (DPN). The values represent the mean ± standard deviation (S.D.) from three independent experiments performed in duplicate. *, $p < 0.05$; **, $p < 0.01$; unpaired *t*-test.

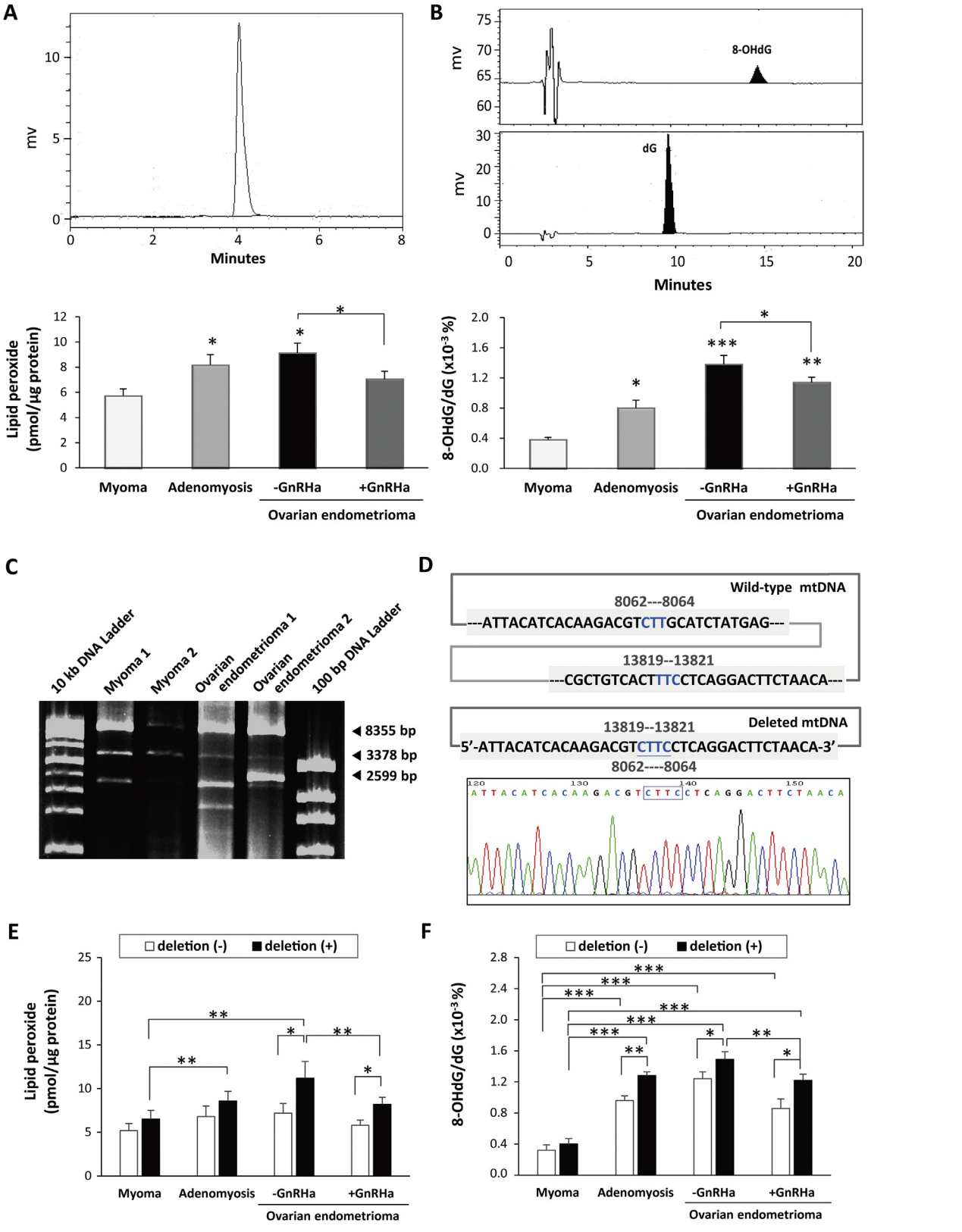

(caption on next page)

at a flow rate of 1 ml/min. The eluent was monitored with a fluorescence detector with the excitation wavelength at 525 nm and emission wavelength at 550 nm.

2.7. Detection of 8-hydroxy-2′-deoxyguanosine (8-OHdG)

An aliquot of 100 μg of DNA was digested by incubation with 1 μl of DNase I (20 units/μl) and 11 μl of a 0.1 M $MgCl_2$ solution at 37 °C for 30 min. After adjusting the pH to 5.0 by adding 1 M sodium acetate and

Fig. 2. Endometriotic lesions show increased accumulation of oxidative damages and mitochondrial DNA deletions. (A) The quantitative analysis of malondialdehyde (MDA) and (B) 8-hydroxy-2′-deoxyguanosine (8-OHdG) were carried out by HPLC-fluorometric detection and HPLC-electrochemical detection to represent oxidative damages on lipid and DNA, respectively. Increased levels of oxidative damages were found in the endometriotic tissues, and a reduction in the ovarian endometriotic tissues from the patients who received GnRH agonist therapy (GnRHa (+)) prior to surgical extraction. (C) Agarose gel electrophoretogram for the multiple mitochondrial DNA (mtDNA) deletions in various human tissues by the long range PCR was shown. Using primer-pair L7901-H16255, three major types of PCR products were generated. The 8355 bp fragment was produced from the wild-type mtDNA, the 3378 bp fragment was from 4977 bp deleted mtDNA, and the 2599 bp fragment was from the 5756 bp deleted mtDNA. (D) A scheme illustrating the occurrence of 5756 bp deletion. DNA sequence in light strand of mtDNA showing the junction site of the 5′-end of the fusion transcript of the 5756 bp deleted mtDNA in human ovarian endometrioma. It revealed a three nucleotide direct repeat (5′-CTT-3′) located at the junction site at nucleotide position (np) 8062–8064 or np 13819–13821 (5′ to 3′) on the light strand DNA. (E) Comparison of the levels of lipid peroxide and (F) 8-OHdG in the endometriotic tissues with or without mtDNA deletion was performed. "Deletion (+)" indicated the endometriotic tissues harboring 4977 bp deleted mtDNA or 5756 bp deleted mtDNA. The values represent the mean ± S.D. from three independent experiments performed in duplicate. *, $p < 0.05$; **, $p < 0.01$. ***, $p < 0.001$ by unpaired *t*-test.

0.1 M $ZnSO_4$. The DNA was hydrolyzed with 1.6 units of nuclease P1 at 65 °C for 10 min, and then hydrolyzed by incubation with 5 units alkaline phosphatase for 30 min at 37 °C. Processed DNA samples were separated on a C18 column on an HPLC system (Jasco) connected in series with an electrochemical detector (Bioanalytical Systems, West Lafayette, IN, USA) and a UV detector set at 254 nm. Elution was performed at a flow rate of 0.8 ml/min for 40 min, with the mobile phase consisting of 12.5 mM citric acid, 25 mM sodium acetate, and 10 mM acetic acid containing 6% methanol (pH 5.8). The amount of 8-OHdG in the DNA sample is expressed as a percentile relative to the amount of the total dG.

2.8. Mitochondrial fractionation

Mitochondria were isolated from the human primary endometrial cells and the human endometriotic tissues by using centrifuge method. In brief, cells were suspended in 1 ml isolation buffer (3 mM HEPES-KOH (pH 7.2), 0.5 mM EGTA, 0.5 mM EDTA, 250 mM sucrose) plus protease inhibitor cocktail. Cells were homogenized using a glass-on-Teflon homogenizer on ice. Cell suspension were centrifuged twice at $800 \times g$ for 10 min at 4 °C to remove cellular debris and nucleus, and the supernatant was centrifuged at $10000 \times g$ for 15 min at 4 °C to pellet mitochondria. The pellets were crude mitochondrial fraction, and the supernatant was defined as cytosolic fraction.

2.9. Western blotting

For western blotting, cells were collected and proteins were extracted by homogenization in lysis buffer (50 mM Tris-HCl (pH 7.4), 15 mM NaCl, 1% PMSF, and 0.1% NP-40), and protease inhibitor cocktail. Fifty micrograms of protein were loaded in SDS-polyacrylamide gels and transferred to PDVF membranes (Millipore, Merck KGaA, Darmstadt, Germany). The membranes were saturated by 5% nonfat milk in TBST, and blotted for molecules of interest with primary antibodies overnight. Bound primary antibodies were detected using appropriate horseradish peroxidase conjugated secondary antibodies followed by detection with ECL™ (GE Healthcare Bioscience). Mean densitometry data from independent experiments were quantified by image analysis software (ImageJ, NIH, USA) and normalized to internal loading control.

2.10. Plasmid transfection

Cells were transfected with pDsRed2-Mito (Clontech Laboratories, Palo Alto, CA, USA), pMito-ERβ, (tERβ) (Plasmid 11352, Addgene, Cambridge, MA, USA), shRNAs targeting ERβ (Academia Sinica, Taipei, Taiwan) or with pcDNA3.1 (scramble shRNA) using Lipofectamine™ 2000 (Invitrogen) following the manufacturer's protocol. The oligo sequence of ERβ-shRNA is CCTTAATTCTCCTTCCTCCTA. The pMito-ERβ was created by inserting ERβ gene (source sequence: BC024181) into pDsRed2-Mito by digestion with BamHI (NEB #R3136, New England Biolabs GmbH, Frankfurt am Main, Germany).

2.11. Immunofluorescence imaging

To identify mitochondrial ERβ localization, triple staining of Dy488-conjugated ERβ, MitoTracker Red (mitochondria-specific probe), and DAPI (nuclear marker) were performed. In brief, cells were fixed in 4% paraformaldehyde, permeabilized by 0.1% Triton X-100, saturated with BSA for 1 h and processed for immunostaining with primary antibodies, anti-ERβ. Cells were incubated with optimized Dy488-conjugated secondary antibodies (1:500, Jackson ImmunoResearch Laboratories, West Grove, PA, USA) followed by primary antibodies overnight. After washing, cells were incubated with MitoTracker Red for 10 min, and mounted with Fluoromount-G™ (Thermo Fisher Scientific) and examined with confocal fluorescence microscope (TCS SP5; Leica Microsystems CMS GmbH, Mannheim, Germany). Confocal fluorescent images were captured using the Leica SP5 confocal microscope fitted with an Apochromat 63 × 1.4 NA immersion objective with three lasers (argon, 488 nm; helium/neon, 543 nm; diode, 405 nm).

2.12. Cellular ROS levels and mitochondrial membrane potential measurement

JC-1 (Thermo Fisher Scientific), can be used as an indicator of mitochondrial potential with emission at 529 nm for JC-1 monomer (green) to 590 nm for JC-1 aggregate (red)) was used to determine mitochondrial membrane potential ($\Delta\psi m$). MitoSOX™ Red (Ex/Em = 510/580 nm, Thermo Fisher Scientific) is a highly selective fluorescent probe dye for mitochondrial superoxide (O_2^-) detection. Intracellular hydrogen peroxides were stained with CM-H_2DCFDA (DCFDA, Thermo Fisher Scientific) and measured using a 490–500 nm wavelength for excitation and 525 nm for emission. Flow cytometric analysis was performed on 10,000 viable cells with FACScan instrument (BD Biosciences FACScan system).

2.13. Cellular ATP content

Absolute ATP contents of treated cells were assayed using the ATPlite™ Luminescence Assay (PerkinElmer). The absolute value of ATP was calculated from a standard curve generated for each individual experiment using serial ATP standards (0 nM–10 mM) and normalized by cell numbers of each individual sample. ATP content was expressed as pmole ATP per 10^4 cells or nmole ATP per mg protein.

2.14. Analysis of mitochondrial oxygen consumption

To investigate the impact of E2 and DPN treatment on cellular metabolic flux activity, intact cellular respiration was detected by Seahorse XF-24 Metabolic Flux assay (Seahorse Bioscience, Agilent, Santa Clara, CA, USA). Oxygen consumption rates of human primary endometriotic cells or mtsERβ overexpressing clones were performed according to the manufacturer's instruction. Briefly, cells were seeded into XF24 cell culture microplates (Seahorse Bioscience) at 40,000 cells/well and incubated at 37 °C and 5% CO_2. Before measurements were made, growth medium was replaced with assay

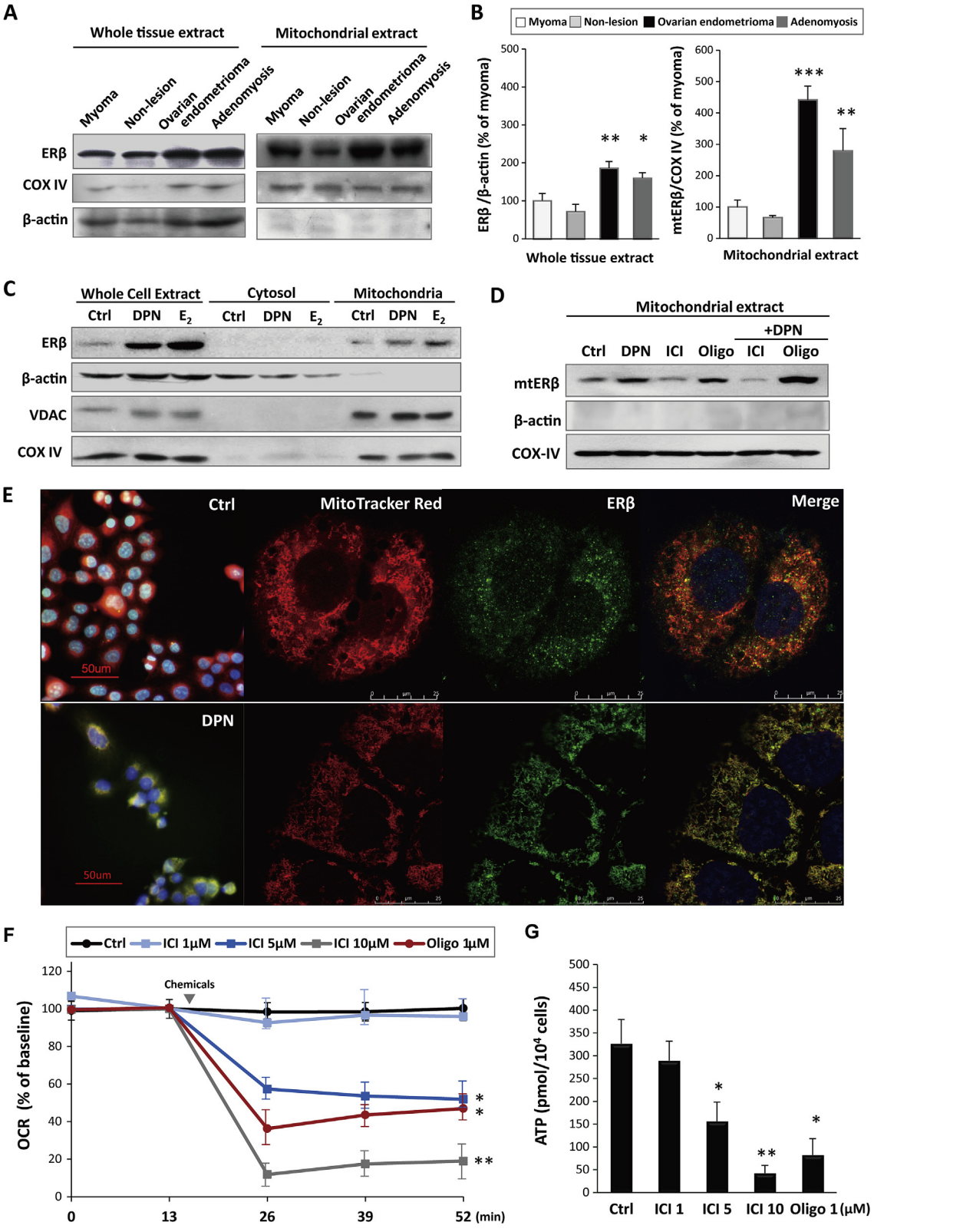

(caption on next page)

medium (phenol red-free and serum-free DMEM/F12 medium without sodium bicarbonate). Oxygen consumption rates (OCR) values are normalized to mg/protein. Baseline measurements were recorded before differential additions of 1, 5, 10 μM ICI 182780, or 1 μM oligomycin.

2.15. Mitochondrial DNA immunoprecipitation (MTDIP)

To detect possible interactions between mtDNA and ERβ, hormone-deprived cells were obtained from the mitochondrial fractionation. MTDIP procedures were performed according to Achanta group [25]. Mitochondria were isolated and cross-linked, then subjected to

Fig. 3. ERβ ligand and metabolic stress recruit ERβ into mitochondria. (A) Representative western blots of ERβ in the whole tissue extracts and mitochondrial extracts of the endometriotic tissues were shown. Greater ERβ levels were detected in the mitochondria of the human endometriotic tissues. Cytochrome *c* oxidase subunit IV (COX IV) was used as the mitochondrial marker, and β-actin, as the cellular and cytosolic marker. (B) Quantitative representations of ERβ distribution in whole tissue and mitochondrial extracts relative to the respective controls were shown. (C) Western blot analysis of ERβ in the following cellular fractions of human endometriotic cells: whole cell extracts, cytosolic extracts and mitochondrial extracts were performed. E2 and DPN markedly enhanced mitochondrial accumulation of ERβ. (D) Western blots of ERβ in the mitochondrial extracts were presented. Higher levels of mtERβ found upon oligomycin treatment without ligand activation. ICI 182780 (ICI) blocked the recruitment of ERβ to mitochondria. (E) Immunofluorescent images of for ERβ (Dy488 conjugated anti-ERβ, green) with mitochondria (MitoTracker Red, red) were visualized in the endometriotic cells treated with or without DPN (ERβ agonist). Scale bar, 25 μm. (F) The mitochondrial oxygen consumption was assessed using Seahorse XF24 Metabolic Flux Analyzer. Data was represented by time courses of the oxygen consumption rate (OCR) under ER antagonist (ICI 182780) or oligomycin treatment. (G) Adenosine triphosphate (ATP) content was measured by ATPlite Luminescence Assay System ICI 182780 inhibited oxygen consumption and ATP synthesis in a dose-dependent manner. The values represent the mean ± S.D. from three independent experiments performed in duplicate. *, $p < 0.05$; **, $p < 0.01$ by unpaired *t*-test. (For interpretation of the references to colour in this figure legend, the reader is referred to the Web version of this article.)

immunoprecipitation (IP) with anti-ERβ antibody (H-150, Santa Cruz Biotechnology). Precipitated DNA was extracted from immunoprecipitation by Qiagen PCR purification kit. Primers, L258-H640 or L15997-H640 for MTDIP-PCR validation of mitochondrial D-loop region for ERβ prospective binding site were the following: L258, 5′-CAGCCACTTTCCACACAGAC-3′, L15997, 5′-CACCATTAGCACCCAA AGCT-3′ and H640, 5′-GGGGTGATGTGAGCCCGTCT-3'. The clinical tissue results were calculated as follows: values obtained from ERβ-precipitated mtDNA were divided by values obtained from mtDNA input, and the ratio normalized with myoma average levels.

2.16. Immunoprecipitation

For immunoprecipitation, cells were lysed in buffer A containing 50 mM Tris·HCl pH 7.6, 150 mM NaCl, 0.5% NP-40, 1% sodium deoxycholate and protease inhibitor cocktail. Cell lysates were pre-cleared with protein G magnetic beads (GE Healthcare Bioscience, Malmö, Sweden) for 30 min. The supernatants were incubated with primary antibody overnight at 4 °C. Then protein G magnetic beads were added and the mixture was further incubated for 2 h at 4 °C. The beads with bound proteins were washed for 6 times with lysis buffer and then boiled in 2X SDS sample buffer, then the resultant samples were detected by Western blotting.

2.17. Annexin V/propidium iodide (PI) assay

Apoptotic cells were identified by staining with Annexin V-FITC conjugate using the TACS™ AnnexinV-FITC apoptosis detection kit (R& D Systems, Minneapolis, MN). Aliquot of 1×10^5 cells were collected, washed, and incubated with 100 μl of binding buffer containing 1 μl of Annexin V-FITC and 10 μg/ml PI for 15 min, after which, 400 μl binding buffer was added. Minimum of 2×10^4 cells were analyzed by flow cytometry as described above. Cells that stained neither with PI nor with Annexin V were considered viable cells.

2.18. Statistical analysis

Data represent mean ± standard deviation (S.D.) of at least three independent experiments. Statistical significance was assessed by two-tailed unpaired Student's-t test. Asterisk(s) indicate significance, *, $p \leq 0.05$; **, $p \leq 0.01$; ***, $p \leq 0.001$. The significance was calculated by inter-group and intra-group comparison.

3. Results

3.1. ERβ level is increased in the endometriotic tissues

We determined the mRNA levels of epithelial (*E-cadherin*) and mesenchymal (*N-cadherin* and *vimentin*) marker genes in the endometriotic tissues for observing the metaplasia properties. The relative change of *N-cadherin*, *E-cadherin* and *vimentin* in different group was compared to the *N-cadherin* expression level of non-lesion group. Comparing with non-lesion, a significant decrease of *E-cadherin* and a significant increase of *N-cadherin* and *vimentin* mRNA was detected in the tissues of adenomyosis and ovarian endometrioma ($p < 0.05$) (Fig. 1A). We measured the mRNA levels of *ERβ* in the endometriotic lesions among patients with endometriosis. Comparing with myoma, a 7.6-fold and 9.3-fold increase of *ERβ* mRNA was detected in the tissues of adenomyosis and ovarian endometrioma ($p < 0.05$) (Fig. 1B). Further to investigate whether ligand-mediated ERβ stimulate endometriotic cell migration, we isolated the primary cells from the dissociated endometriotic tissues and variously treated with E2, DPN (the highly selective agonist of ERβ), or ICI 182780 (ER antagonist). More mesenchymal-like morphology and higher migration capacity was observed in the estradiol-primed endometriotic cells (Fig. 1C and D). We further found that the ICI 182780, which interferes with ligand binding to ERα and ERβ, mitigated the estradiol-induced mesenchymal-like morphological changes and endometriotic cell migration (Fig. 1C and D).

3.2. Endometriotic lesions show increased accumulation of oxidative damages and mitochondrial DNA deletions

To examine whether the oxidative damages accumulated in endometriotic lesions, we analyzed the formation of lipid peroxides and 8-OHdG. MDA is a byproduct of lipid oxidation by ROS, and this aldehyde reacts readily with protein or DNA forming MDA-protein or MDA-DNA adducts which are considered highly toxic. Lipid peroxidation in endometriotic tissues was assessed by quantifying MDA. The highest levels of lipid peroxidation were found in the ovarian endometrioma tissues (Fig. 2A). The oxidative damage to genomic DNA of endometriotic tissues were investigated by measuring 8-OHdG, one of the base modifications by ROS (Fig. 2B). A statistical significantly higher levels of MDA and 8-OHdG were found in the patients with endometriosis, whereas reduction of oxidative damages on the lipid and DNA whom received the GnRHa therapy for 3 months (Fig. 2A and B). It implies that oxidative damages are contributing to the progression of endometriosis.

ROS overproduction is believed to be the important cause of mtDNA mutations. We further measured the occurrence of mtDNA deletions in the endometriotic tissues by long range PCR. Using primer-pair L7901-H16255, three major types of PCR products were obtained. The 8355 bp fragment was produced from the wild-type mtDNA, the 3378 bp fragment was from 4977 bp deleted mtDNA, and the 2599 bp fragment was from the 5756 bp deleted mtDNA (Fig. 2C). DNA sequencing revealed a three nucleotide direct repeat (5′-CTT-3′) located at the junction site at np 8062–8064 (5′ to 3′) or np 13819–13821 (5′ to 3′) on the light strand DNA of the 5756 bp deleted mtDNA (Fig. 2D). Moreover, the higher levels of MDA and 8-OHdG were found in the endometriotic tissues harbored mtDNA 4977 bp deletion or the 5756 bp deletion (Fig. 2E and F).

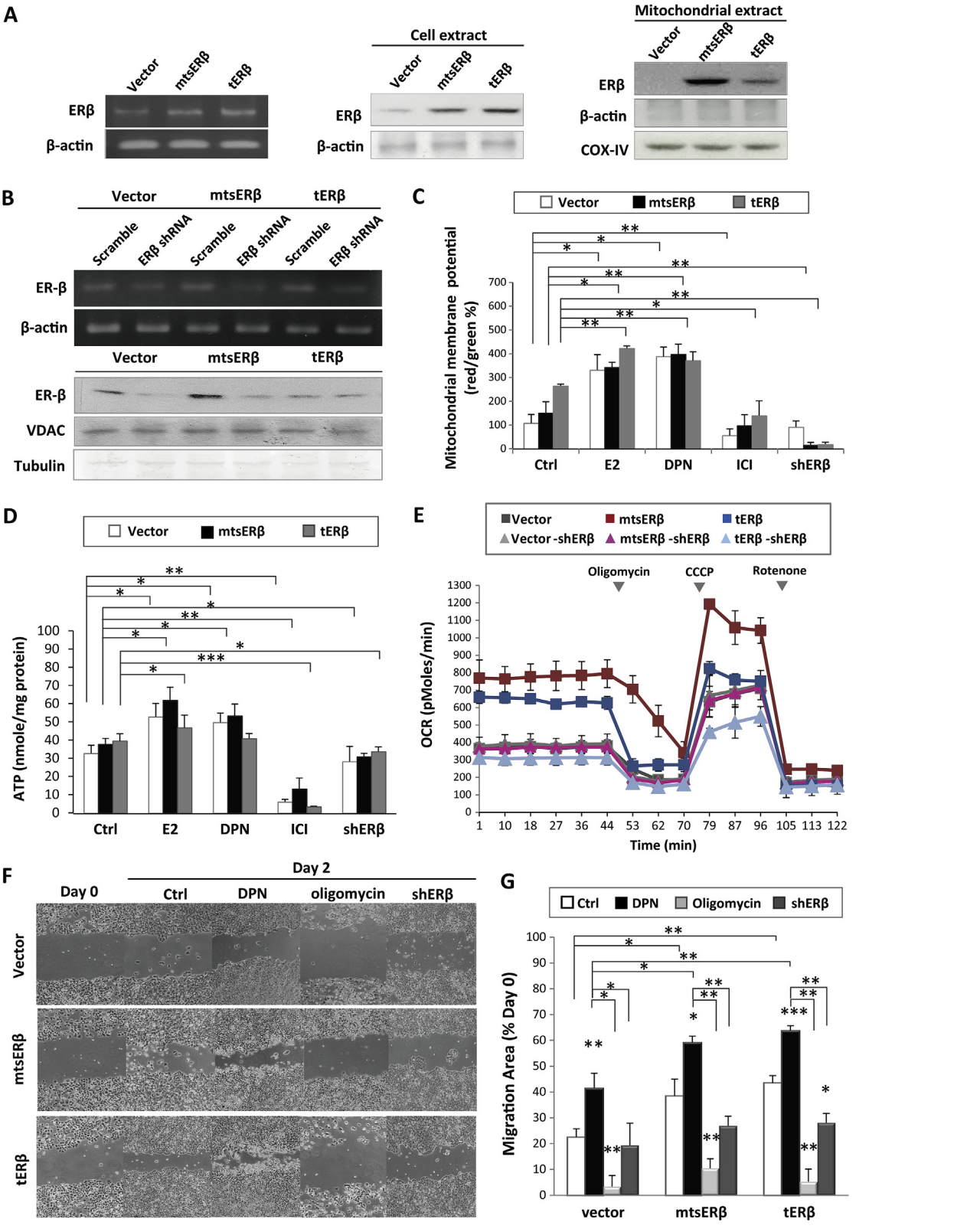

(caption on next page)

3.3. ERβ ligand and metabolic stress recruit ERβ into mitochondria to increase mitochondrial bioenergetics

To test whether ERβ accumulated in a new subcellular pool, mitochondria, we isolated the mitochondrial fraction from the human ectopic endometriotic tissues. Through western blotting, we showed the enhanced levels of mitochondrial ERβ (mtERβ) in different types of endometriotic tissues (adenomyosis and ovarian endometrioma) compared with uterine myoma or non-lesion controls (Fig. 3A). The levels of mtERβ in the endometriotic tissues were significantly higher than the comparative controls (Fig. 3B). To investigate whether ligand-mediated ERβ activation required for mitochondrial translocation of ERβ, human

Fig. 4. Overexpression of mitochondrial-targeting ERβ enhanced mitochondrial bioenergetics and contributed to endometriotic cell migration. (A) The electrophoretograms and western blots of ERβ in control vector (vector), mitochondrial specific ERβ-overexpressing (mtsERβ) and total ERβ-overexpressing (tERβ) cells were presented. The mtsERβ clone displayed the specific mitochondrial localization of ERβ. COX IV was used as the mitochondrial marker, and β-actin, as the cellular and cytosolic marker. (B) The knockdown efficiency of ERβ with short hairpin RNA (shRNA) by western blotting was demonstrated. (C) The effect of ICI 182780 and ERβ-shRNA on the mitochondrial membrane potential of the vector, mtsERβ and tERβ clones were stained with JC-1 and assessed using flow cytometry. (D) The effect of ICI 182780 and ERβ-shRNA on the ATP generation was measured by ATPlite Luminescence Assay System. ICI 182780 and ERβ-shRNA dissipated mitochondrial membrane potential and ATP synthesis. (E) The oxygen consumption rate (OCR) of the ERβ-overexpressing or ERβ-deficient clones were assessed by the sequential addition of 1 μM oligomycin, 1 μM CCCP, and 3 μM rotenone using Seahorse XF24 Metabolic Flux Analyzer. (F) Representative images of cell migration by scratch assay were shown for vector, mtsERβ and tERβ clones. The mtsERβ and tERβ clone exhibited higher migration ability. (G) The percentages of wound area were normalized with the area at 0 h, and vary with the treatments. Oligomycin and ERβ-shRNA inhibited the cell migration of the three clones. The values represent the mean ± S.D. of at least three independent experiments performed in duplicate. *, $p < 0.05$; **, $p < 0.01$; ***, $p < 0.005$ vs. control group or intergroup vector cell.

primary endometriotic cells were variously treated with E2 and DPN. A greater than two-fold increase of mtERβ was found in with 10 nM E2 or 10 nM DPN treatment compared with untreated control, with marked changes in total ERβ of whole cell extract (Fig. 3C).

We further found that endogenous ERβ was recruited to the mitochondria upon oligomycin treatment without ligand activation (Fig. 3D). However, the oligomycin-intensified mitochondrial translocation of ERβ was additionally enhanced by co-treatment with DPN. This finding suggests that the ERβ translocation into mitochondria was responded to ATP dissipation. In contrast, ICI182780, which interferes with ligand binding to ERβ, attenuated ERβ mitochondrial translocation, and this effect was not reversed by the later addition of DPN. Thus, the mitochondrial translocation of ERβ was enhanced via ERβ-ligand interaction or mitochondrial stress. Observation of primary endometrium cells stained with MitoTracker Red for mitochondria and immunostained with Dy488 conjugated anti-ERβ, we revealed a major fraction of ERβ with ERβ agonist (DPN) treatment in the mitochondria (Fig. 3E). Thus, both ER ligand and ERβ agonist can facilitate the translocation of ERβ into mitochondria.

To further evaluate the bioenergetic alterations subsequent to ER antagonist treatment, we used the Seahorse XF-24 Analyzer to assess mitochondrial oxygen consumption rate (OCR). As shown in Fig. 3F, comparing ICI 182780 with oligomycin in the primary endometriotic cells, the demonstrated dose-response reduction in OCR with ICI 182780 suggested that the ER antagonist might be a potential respiration inhibitor. Additionally, a dose-depend decline of ATP content with ICI 182780 treatment were represented (Fig. 3G). The induced mitochondrial translocation of ERβ by mitochondrial metabolic stress renders ERβ in response to the mitochondrial bioenergetics.

3.4. MtERβ involves in the maintenance of mitochondrial function

To investigate whether the effects of mtERβ on mitochondria via ligand-dependent or independent activation, we established a cell model for the direct trafficking of ERβ to the mitochondria. Endometriotic cells were established overexpressing ERβ with a mitochondrial targeting sequence (mts) based on pDsRed2-Mito vector (mtsERβ). Similarly, cells cloned with pRST-ERβ overexpressed total ERβ (tERβ) (Fig. 4A). The immunoblotting results showed that ERβ was localized to the mitochondria in mtsERβ and tERβ clones. Significantly, mtsERβ clones presented predominant mitochondrial localization of ERβ without exogenous ligand activation (Fig. 4A).

To understand how mtERβ affects mitochondrial function, we monitored Δψm and ATP content in the mtERβ overexpressing and knockdown clones. The knockdown efficiency of ERβ with short hairpin RNA (shRNA) by western blotting was shown in Fig. 4B. ERβ-specific shRNA constructs efficiently knocked down ERβ expression in mtsERβ and tERβ clones. Among the three clones without exogenous ligands, mtsERβ and tERβ clones had significantly higher Δψm (Fig. 4C). E2 and DPN significantly enhanced Δψm in all clones; in contrast, ER antagonists and knockdown of ERβ significantly reduced Δψm. Additionally, we quantified the alteration of ATP content with treatment in E2, DPN, ICI 182780 and ERβ knockdowns. E2 and DPN treatments significantly increased ATP generation, and these were dependent upon ERβ, as demonstrated by ICI 182780 and ERβ knockdown (Fig. 4D). To further evaluate the bioenergetic alterations subsequent to mtERβ translocation, we used the Seahorse XF-24 Analyzer to monitor cellular respiration profiles of ERβ-overexpressing clones. Strikingly, an increase in basal respiration, reserved respiratory capacity and proton production rate, and a decrease in proton leak were observed in mtsERβ clones (Fig. 4E and Supplementary Fig. 1). The knockdown of ERβ significantly attenuated Δψm, ATP generation, and mitochondrial respiration without exogenous ligands, thereby recapitulating the ligand-independent ERβ effect on mitochondrial functions.

In addition to understand whether the enhanced energy production contribute to promoting endometriotic cell migration, we examined the cell migratory ability of the differential ERβ clones by scratch assay. Representative images of cell migration were shown for vector-only, mtsERβ and tERβ clones in Fig. 4F. The mtsERβ and tERβ clone exhibited higher migration ability in ligand-independent and ligand-depend manner. The migration area was measured after 48-h treatment with 10 nM DPN or 1 μM oligomycin, or transfected with scramble or ERβ-shRNA. A specific inhibitor of ATP synthase, oligomycin, significantly inhibited the migration of the three clones. The specific knockdown of ERβ by ERβ-shRNA modestly reduced the migration area in the tERβ clone compared to oligomycin (Fig. 4G). The inhibition of ATP production prohibited endometriotic cell migration implicated the relations among mitochondria, ERβ, and endometriosis.

3.5. MtERβ integrates mtDNA replication and transcription to induce mitochondrial biogenesis

To address whether ERβ-mediated induction of mtDNA-encoded mitochondrial respiratory complex (MRC) proteins without ligand activation, we found a remarkable increase in mitochondria-encoded MRC Complex IV proteins in the mtsERβ clones. Knockdown of ERβ significantly diminished the synthesis of mtDNA-encoded complex IV in mtsERβ clones compared with scramble shRNA controls (Fig. 5A). The mtsERβ clones also exhibited a higher amount of mitochondrial transcribed *mt-CO1* (Complex IV subunit 1) and *mt-ATP6* (Complex V subunit 6), which is indicative of an increase in mitochondrial transcription (Fig. 5B). Therefore, mtERβ was directly responsible for the synthesis of mtDNA-encoded MRC complex IV, independent of ligand activation.

To further understand whether ERβ regulates mtDNA gene expression via upregulation of NRF-1, which regulates TFAM, we observed the increased *NRF-1* and *TFAM* transcripts and protein levels in mtsERβ and tERβ clones, whereas the ERβ knockdown decreased *NRF-1* and *TFAM* transcripts and protein levels (Fig. 5C). In mitochondria, mtDNA D-loop region has partial sequence similarity with estrogen response element (ERE), suggesting the possibility of direct binding by mtERβ to mtDNA to regulate mitochondrial gene expression. We showed an increased interaction between mtERβ and mtDNA D-loop region at nucleotide position (n.p.) 15997 and n.p. 640 in the mtsERβ clone and the endometriotic tissues using mitochondrial DNA immunoprecipitation (MTDIP) assay (Fig. 5D and E). The lack of mtDNA PCR fragments in nonspecific IgG samples demonstrated the high specificity of

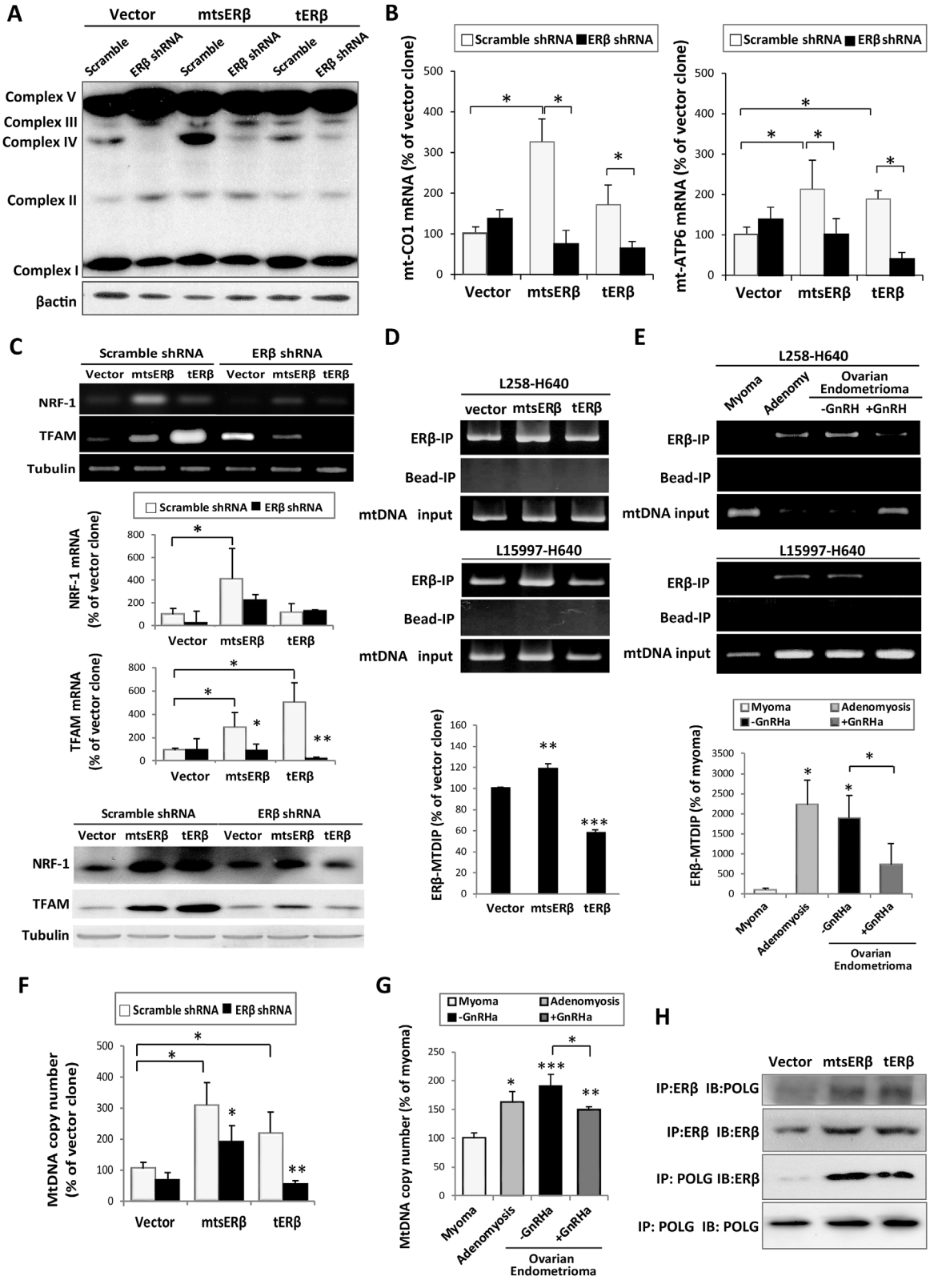

(caption on next page)

immunoprecipitation by ERβ. The mtsERβ clone exhibited a greater ERβ-mtDNA interaction compared to the tERβ clone (Fig. 5D and E). Adenomyosis and ovarian endometrioma without GnRHa therapy exhibited greater ERβ-mtDNA interaction than in myoma, as quantified by real-time qPCR. GnRHa therapy reduced this interaction (Fig. 5E).

Concurrently, we found a notable increase in mtDNA content (copy number) for both mtsERβ and tERβ clones by real-time qPCR (Fig. 5F). Knocking down ERβ in these clones significantly mitigated the mtDNA levels of both clones, indicating that ERβ involves in mtDNA replication. Consistently, the mtDNA content was elevated in the ovarian endometrioma samples and declined in patients who received GnRHa therapy for 3 months (Fig. 5G). GnRHa therapy suppressed estrogen

Fig. 5. MtERβ integrates mtDNA replication and transcription to induce mitochondrial biogenesis. (A) Antibody cocktail (MS604) against mitochondrial complexes was used to examine the expression profiles of mitochondrial respiratory complexes. Five distinct bands were represented as Complex I subunit NDUFB8 (~20 kD), Complex II subunit FeS (30 kD), Complex III subunit Core 2 (~47 kD), Complex IV subunit I (~39 kD), and ATP synthase subunit alpha (53 kD) in the immunoblot. The mitochondria-encoded respiratory complex IV proteins was increased in the mtsERβ clones, and decreased by ERβ-shRNA. (B) The levels of mitochondria-encoded gene transcripts, *mt-CO1* and *mt-ATP6* transcripts, were determined by real-time qPCR. (C) The transcript levels and protein levels of mtDNA transcription factors, nuclear-derived nuclear respiratory factor 1 (NRF-1) and mitochondrial transcription factor A (TFAM), were analyzed by real-time qPCR and western blot, respectively. (D) The electrophoretograms represented that mtERβ binds to the mtDNA D-loop region, as assayed by mtDNA immunoprecipitation (MTDIP)-PCR assay using primer pairs L258-H640 and L15997-H640. The interaction between mtERβ and the mtDNA D-loop region was determined in the mitochondrial extracts of vector, mtsERβ and tERβ clones. The following fractions were tested for mtDNA: ERβ-IP, immunoprecipitation with anti-ERβ antibody; Bead-IP, immunoprecipitation with bead-conjugated IgG; and mtDNA, total mtDNA before immunoprecipitation, which served as an input control. (E) The interaction between mtERβ and mtDNA of the endometriotic tissues was performed using MTDIP-PCR assay. Ovarian endometriotic tissues were categorized into patients who received (+) or did not receive (−) GnRH agonist (GnRHa) therapy prior to surgical extraction. (F) The mtDNA copy number was determined by real-time qPCR in the vector, mtsERβ and tERβ clones. (G) The mtDNA copy number was measured in the human endometriotic tissues. (H) The mitochondrial fractions were immunoprecipitated with anti-ERβ antibody or anti-polymerase γ (POLG) antibody and then western blotted against both POLG and ERβ; the results indicate the specific presence of ERβ interacting with POLG within mitochondria. All of the values are expressed as the means ± S.D. from three independent experiments performed in duplicate. *, $p < 0.05$; **, $p < 0.01$; ***, $p < 0.005$; unpaired *t*-test.

production, implying that mtDNA replication could be regulated by estrogen level. To further understand the regulation of mtERβ on mtDNA replication, we investigated the interactions between mtERβ and polymerase γ (POLG). POLG is essential and specific for mtDNA replication. We found that both mtsERβ and tERβ clones exhibited relatively higher mtERβ-POLG co-immunoprecipitation compared with vector clone (Fig. 5H). Thus, we propose that the increased interactions between ERβ-POLG and ERβ-mtDNA lead to upregulation of mtDNA gene replication.

3.6. MtsERβ enhance the survival of endometriotic cells by sanitizing ROS insults

It is known that elevated mitochondrial respiration and higher proton production concurrently exacerbates mitochondrial ROS generation. The mitochondrial superoxide ($O_2^{\cdot-}$) and intracellular hydrogen peroxide in vector-only, mtsERβ and tERβ clones with and without DPN were determined. The mtsERβ and tERβ clones exhibited lower superoxide production in mitochondria (Fig. 6A). DPN treatment further attenuated ROS generation in the three clones (Fig. 6B). We further examined whether the lower ROS levels in the mtsERβ clone might be partly due to the induction of ROS scavenger enzymes. MnSOD, a mitochondrial-matrix-localized redox enzyme, is the major ROS scavenger within mitochondria. ERβ-induced MnSOD elevation was further confirmed by ERβ knockdown which markedly diminished the MnSOD transcript level in mtsERβ and tERβ clones (Fig. 6C and D). Thus, ERβ regulates MnSOD expression and the scavenging of superoxide by MnSOD may alleviate ROS stress, thereby enhancing the resistance to ROS-induced cell death.

In addition to realize the mitochondrial roles in energy generation and oxidative stress response signaling, mitochondria are the focal points of key events in cell apoptosis. Therefore, we addressed whether mtERβ protected cells from ROS-induced cell death. The proportion of non-apoptotic cells (PI negative and AV negative) for the three clones treated with 10 nM, 100 nM and 200 nM H_2O_2 were determined by Annexin V-PI assay (Fig. 7A and B). Vector-only clone showed higher proportion of cell apoptosis, augmented cytochrome *c* release from mitochondria to cytosol, and increased caspase-3 activation compared to mtsERβ and tERβ clones after exposure to 100 nM H_2O_2 (Fig. 7B, C, and D). As expected, the mtsERβ and tERβ clones were more resistant to ROS-induced apoptosis compared to vector-only clone. Moreover, under resting conditions, mtsERβ and tERβ clones exhibited higher levels of anti-apoptotic protein Bcl-2 (Fig. 7D). These results suggest that ERβ increases intracellular Bcl-2, thereby rescuing cells from oxidative stress-induced mitochondrial apoptosis signaling pathway.

4. Discussion

Endometriosis is regarded as a premenopausal disease. High levels of ERβ in endometriosis are considered to play an aggravated role in the pathogenesis of endometriosis. Natural and iatrogenic menopause resolves the disease progression due to the lower levels of estrogen. In addition, the weaker ERβ expression than ERα expression has been documented in the atrophic and inactive post-menopausal endometrium [26]. However, the recurrence of endometriosis in the post-menopausal women with hyperestrogenemia was noted [27].

In line with our observations, the elevated ERβ level exhibited in the mitochondrial localization of endometriotic tissues. The ERβ antagonist, ERβ shRNA, and oligomycin-induced dissipation of ATP inhibited endometriotic cell migration implicated the relations among mitochondria, ERβ, and endometriosis. Our findings provide the first evidence that ERβ accumulates in the mitochondria of clinical endometriotic tissues, through ligand activation (estradiol or DPN) or through specific mitochondrial respiratory inhibitor (oligomycin). This study characterizes that mtERβ improves the mitochondrial bioenergetics, and induces direct interaction among mtERβ, mtDNA, and POLG leading to reinforcing mitochondrial gene expression. The specific overexpression of mtsERβ and tERβ strengthen anti-apoptotic potential by reducing ROS through induction of MnSOD and Bcl-2 expression. Thus, mtERβ is proposed to have cell-protective effects by maintaining mitochondrial function and sanitizing the oxidative damages to facilitate ectopic endometriotic cell survival.

Endometriosis is believed to increase the risk of developing ovarian cancer [3,28] and endometrial cancer [2]. The ovarian endometrioma was associated with a 2.6 fold increased risk for ovarian cancer [28]. These investigations support the hypothesis that ERβ may function as a tumor suppressor in carcinogenesis. However, there are increased evidences showed that the extraordinarily higher level of ERβ and significantly lower level of ERα in the endometriotic stromal cells [29–32]. Overexpressed ERβ in endometriosis has been depicted to represent the broad effects on endometriotic cells, such as facilitating cell cycle progression and proliferation, inducing cyclooxygenase 2 expression and prostaglandin biosynthesis, and failure to induce progesterone receptor expression response to estradiol stimulation [12,30].

The high level of ERβ in various diseases are responsible for a wide variety of vital cellular processes including in cellular metabolism and mitochondrial bioenergetics affecting cellular proliferation and apoptotic potential [19]. Both nuclear and cytoplasmic distributions of ERβ have been identified to promote ectopic lesion survival. The nuclear-localized ERβ exhibits the transcriptional activation of the serum and glucocorticoid-regulated kinase to inhibit cell apoptosis [33], and cytoplasmic ERβ blocks TNF-α-induced cell apoptosis [34]. Our data show that ERβ translocation into mitochondria is beneficial for estrogen-dependent growth of endometriotic cells that may be involved in the development of endometriosis. The ectopic endometriotic deposits adopt proliferative and apoptosis-resistant phenotypes that have survival advantages at ectopic sites and gives rise to further endometriotic deposits to maintain the disease progression. The ectopic endometriotic

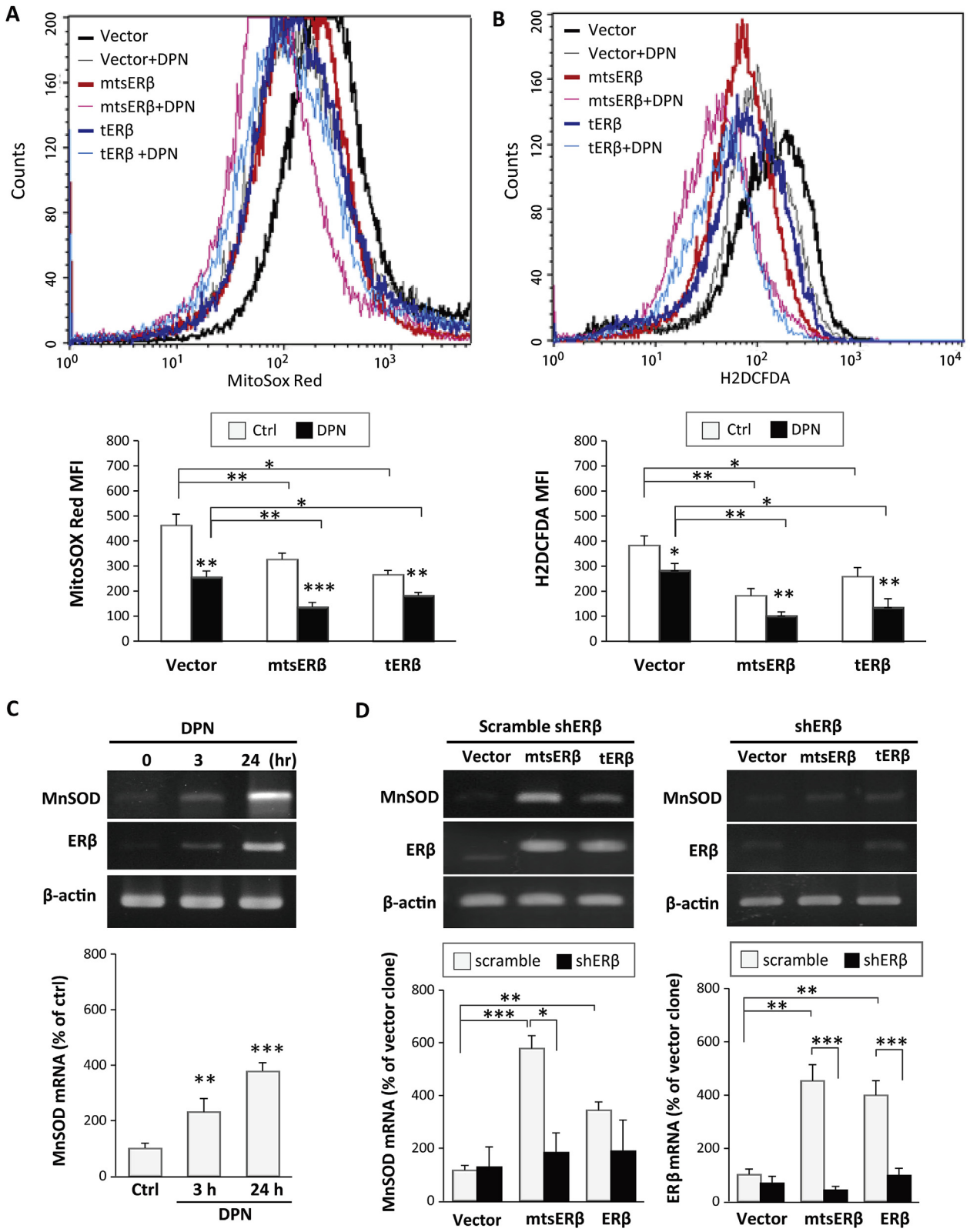

Fig. 6. MtERβ reduced ROS generation and enhanced MnSOD expression. The fluoroprobes, (A) MitoSOX Red and (B) H2DCFDA, were introduced for the selective detection of mitochondrial superoxide and cellular hydrogen peroxide, respectively. Histograms and mean fluorescent intensity (MFI) of MitoSOX Red and H2DCFDA were analyzed in the vector, mtsERβ and tERβ clones. MtsERβ and tERβ clones. (C) Representative electrophoretograms of MnSOD and ERβ transcripts were shown. A time-dependent increase in MnSOD transcript levels in ERβ agonist (DPN) treatment was detected by real-time qPCR. (D) The level of MnSOD transcripts was enhanced in mtsERβ and tERβ clones, but diminished by ERβ-shRNA, as assessed by real-time qPCR. The values represent the mean ± S.D. from three independent experiments performed in duplicate. *, $p < 0.05$; **, $p < 0.01$ by unpaired *t*-test. (For interpretation of the references to colour in this figure legend, the reader is referred to the Web version of this article.)

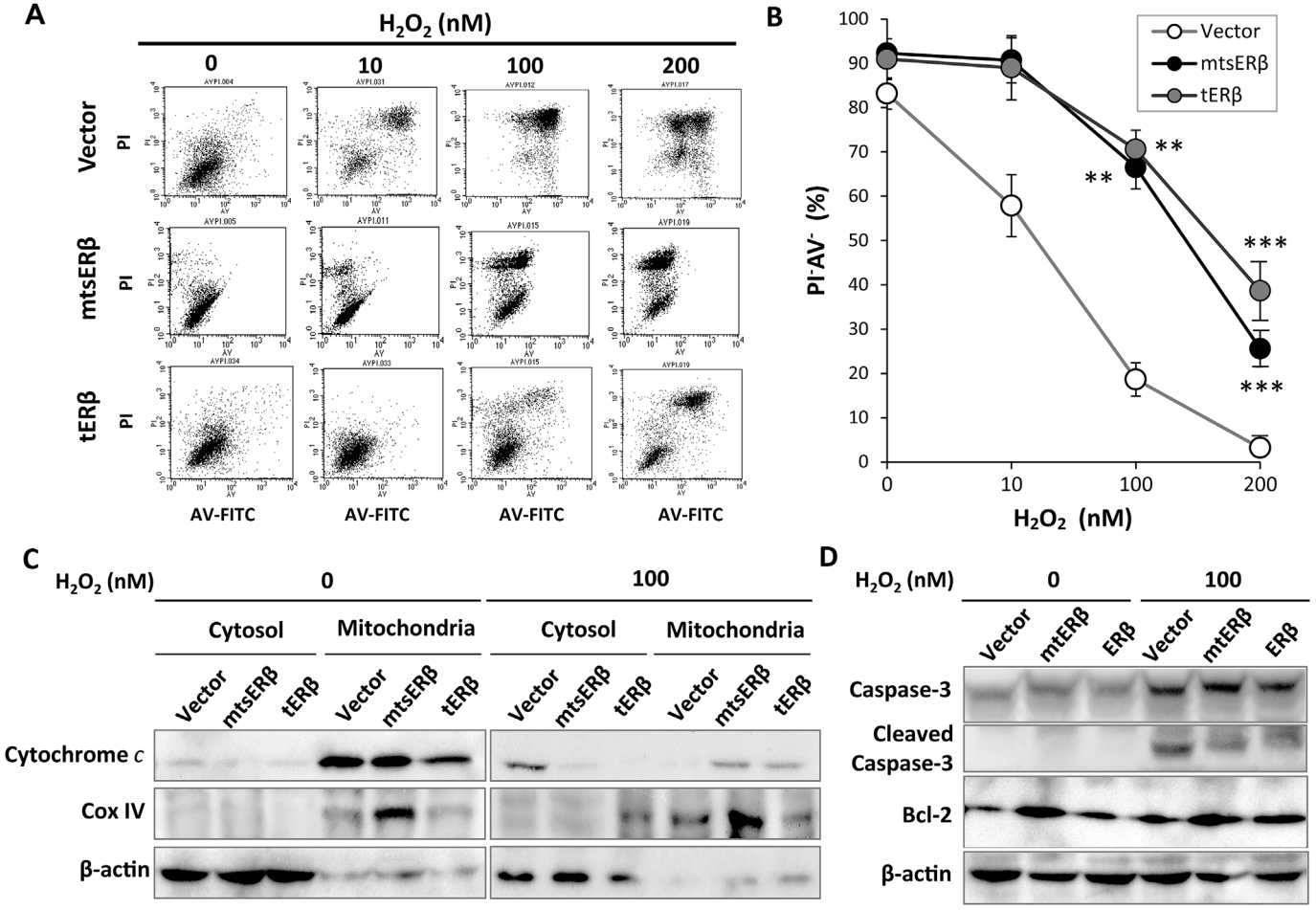

Fig. 7. MtERβ enhance the survival of endometriotic cells by sanitizing ROS insults. (A) Effect of hydrogen peroxide on the vector, mtsERβ and tERβ clones were measured with Annexin V-FITC (green signal) and DAPI (blue signal) staining. The scatter plots of AV-FITC and PI were shown. (B) Percentage of non-apoptotic cells (AV-FITC−/PI−) was obtained using flow cytometry. A dose-dependent reduction of AV-FITC/PI (−/−) in the control vector clones was found that exposure to 0, 10, 100, or 200 nM H_2O_2. The substantial cell death induced by H_2O_2 was significantly reduced in the ERβ-overexpressing cells. The values represent the mean ± S.D. of at least three independent experiments performed in duplicate. **, $p < 0.01$; ***, $p < 0.005$. (C) Representative western blots showing the protein level of cytochrome *c* in the mitochondrial extracts and cytosolic extracts of the three indicated clones with or without 100 nM H_2O_2 treatment. (D) Western blot analysis of caspase-3 and Bcl-2 in the indicated clones that exposure to 0, 10, or 100 nM H_2O_2 was performed. The cytochrome *c* releasing from mitochondria to cytosol and proteolytic activation of caspase 3 induced by H_2O_2 was significantly reduced in the ERβ-overexpressing cells.

deposits induce inflammatory responses and local estrogen overproduction. It also points to the possibility that the ectopic niche may further promote ERβ translocation into the mitochondria to govern mitochondrial integrity, inhibit cell apoptosis, and contribute to the development and progression of endometriosis.

MtERβ is presumed to proceed the estrogen-induced signaling pathway within mitochondria to affect mitochondrial DNA transcription [15,19], and was demonstrated to interact with mitochondrial respiratory complex V and to enhance mitochondrial respiratory complex IV activity [35,36], suggesting a relationship between mtERβ and ATP generation. To understand the effect of mitochondrial targeted ERβ, we engineered a cell model for the direct trafficking of ERβ to the mitochondria. In our observation, mtsERβ clone shows higher ATP production and mitochondrial membrane potential. ERβ antagonist (ICI 182780) and ERβ-shRNA collapses Δψm and dissipates ATP synthesis and mitochondrial oxygen consumption. These findings suggest a pivotal role for mtERβ as a mitochondrial metabolic regulator. The direct regulation by mtERβ of mtDNA transcription may occur through a direct interaction with mtDNA D-loop region. In addition to this direct interaction, the mtERβ-induced mitochondrial retrograde signaling pathway is assumed to induce *NRF-1* and *TFAM* expression, which binds to mtDNA D-loop region to further activate mtDNA expression. Furthermore, increased mtDNA copy number in endometriotic tissues might be due to synergistic compensation in response to mitochondrial energy deficits or the accumulation of mtDNA mutations. Previously, the increased pathogenic mtDNA mutations were discovered in the patients with endometriosis or type I endometrial carcinoma (EC) [23,37]. The occurrence of mtDNA mutations was positively correlated with mtDNA copy number in the EC tumor tissues. The synergistic compensation theory has been proposed in the development of endometrial adenocarcinoma cells [37].

Our work shows that oligomycin induces ERβ translocation into the mitochondria without prior activation by an exogenous ligand in mtsERβ clone. Additionally, mtsERβ clone exhibits a higher respiratory capacity and higher expression level of genes affecting ATP synthesis than parental cells to alleviate oligomycin-mediated mitochondrial dysfunction. Furthermore, the inhibition of ATP production by oligomycin or ERβ shRNA prohibited endometriotic cell migration. Recent study demonstrated that the anterior localization of mitochondria in moving epithelial cancer cells is account for highly migratory phenotype [38]. The ATP generation, ROS production, and mitochondrial calcium signaling is further proposed to be the important regulators for cell migration [39]. Given the importance of mtERβ in regulating mitochondrial bioenergetics responding to energy demand, mtERβ might

contribute to potentiate endometriotic cell migration and disease progression.

Oxidative stress is clearly related to the progression of endometriosis and is considered to destruct the peritoneal mesothelium leading to adhesions for ectopic endometrial cells [40]. Best known for the leakage of electrons from electron transfer chain, mitochondria is the major site of ROS generation. The present results showed that the significantly higher levels of MDA and 8-OHdG were detected in endometriotic lesions than in controlled non-lesion endometrium. Additionally, the occurrence of mtDNA mutations was positively associated with the levels of MDA and 8-OHdG. Previous studies have reported that E2 or ERβ-selective agonist drives the upregulation of MnSOD activity and MnSOD gene expression [41–43]. To test whether ERβ modulate the ROS scavenging system, we fond that ERβ-selective agonist, mtsERβ clone, or tERβ clone induces MnSOD gene expression. It is conceivable that the enhanced MnSOD expression of mtsERβ clone decrease ROS levels and increase the survival of endometriotic cells against ROS insult. Additionally, ERβ has been found to exhibit non-genomic action for anti-apoptosis. Several studies represent the molecular details of ERβ-mediated anti-apoptosis, including interacting with apoptosis signal-regulating kinase 1 to disrupt tumor necrosis factor α (TNFα)-induced apoptosome formation in ectopic lesions [8,34]. Moreover, ERβ interacts with Bad, within mitochondria, to inhibit Bad-Bcl-XL complex formation to promote ectopic cell survival [44]. Here, we found that mtsERβ overexpression afforded an increase of Bcl-2 protein levels. Combined with our results, these findings imply that mtERβ either maintains or protects mitochondrial function to reduce the susceptibility of cells to oxidative stress or metabolic stress.

In conclusion, our results show for the first time that mtERβ may play an adaptive role in the context of the development of endometriosis along with intensified mitochondrial function. MtERβ is responsible for the specific molecular and histological findings of endometriosis. With our increasing understanding of mtERβ in restoration of mitochondrial bioenergetics, a more comprehensive model of mitochondrial genetics and biogenesis should soon emerge; this model, in turn, will contribute to the development of new approaches to maintain healthy mitochondria. The ERβ-selective estrogen receptor modulator may serve as novel therapeutics strategies of endometriosis in the future.

Acknowledgements

This work was supported by Basic Research Grants NSC 96-2320-B-038-009 and NSC 99-2632-B-038-001-MY3, National Science Council, Republic of China. The instruments were provided by the Core Facility Center, Office of Research and Development of Taipei Medical University.

Appendix A. Supplementary data

Supplementary data to this article can be found online at https://doi.org/10.1016/j.freeradbiomed.2019.01.022.

References

[1] S.E. Bulun, Endometriosis, N. Engl. J. Med. 360 (2009) 268–279.
[2] I.J. Rowlands, C.M. Nagle, A.B. Spurdle, P.M. Webb, Gynecological conditions and the risk of endometrial cancer, Gynecol. Oncol. 123 (2011) 537–541.
[3] E. Veras, T.L. Mao, A. Ayhan, S. Ueda, H. Lai, M. Hayran, M. Shih Ie, R.J. Kurman, Cystic and adenofibromatous clear cell carcinomas of the ovary: distinctive tumors that differ in their pathogenesis and behavior: a clinicopathologic analysis of 122 cases, Am. J. Surg. Pathol. 33 (2009) 844–853.
[4] R.J. Kurman, M. Shih Ie, Molecular pathogenesis and extraovarian origin of epithelial ovarian cancer–shifting the paradigm, Hum. Pathol. 42 (2011) 918–931.
[5] A.M. Shaaban, A.R. Green, S. Karthik, Y. Alizadeh, T.A. Hughes, L. Harkins, I.O. Ellis, J.F. Robertson, E.C. Paish, P.T. Saunders, N.P. Groome, V. Speirs, Nuclear and cytoplasmic expression of ERbeta1, ERbeta2, and ERbeta5 identifies distinct prognostic outcome for breast cancer patients, Clin. Canc. Res. 14 (2008) 5228–5235.
[6] Y.J. Chen, H.Y. Li, C.H. Huang, N.F. Twu, M.S. Yen, P.H. Wang, T.Y. Chou, Y.N. Liu, K.C. Chao, M.H. Yang, Oestrogen-induced epithelial-mesenchymal transition of endometrial epithelial cells contributes to the development of adenomyosis, J. Pathol. 222 (2010) 261–270.
[7] S. Matsuzaki, C. Darcha, Epithelial to mesenchymal transition-like and mesenchymal to epithelial transition-like processes might be involved in the pathogenesis of pelvic endometriosis, Hum. Reprod. 27 (2012) 712–721.
[8] S.J. Han, S.Y. Jung, S.P. Wu, S.M. Hawkins, M.J. Park, S. Kyo, J. Qin, J.P. Lydon, S.Y. Tsai, M.J. Tsai, F.J. DeMayo, B.W. O'Malley, Estrogen receptor beta modulates apoptosis complexes and the inflammasome to drive the pathogenesis of endometriosis, Cell 163 (2015) 960–974.
[9] G. Hudelist, J. Keckstein, K. Czerwenka, H. Lass, I. Walter, M. Auer, F. Wieser, R. Wenzl, E. Kubista, C.F. Singer, Estrogen receptor beta and matrix metalloproteinase 1 are coexpressed in uterine endometrium and endometriotic lesions of patients with endometriosis, Fertil. Steril. 84 (Suppl 2) (2005) 1249–1256.
[10] E. Trukhacheva, Z. Lin, S. Reierstad, Y.H. Cheng, M. Milad, S.E. Bulun, Estrogen receptor (ER) beta regulates ERalpha expression in stromal cells derived from ovarian endometriosis, J. Clin. Endocrinol. Metab. 94 (2009) 615–622.
[11] D. Chakravarty, R. Srinivasan, S. Ghosh, S. Gopalan, A. Rajwanshi, S. Majumdar, Estrogen receptor beta1 and the beta2/betacx isoforms in nonneoplastic endometrium and in endometrioid carcinoma, Int. J. Gynecol. Canc. 17 (2007) 905–913.
[12] S.E. Bulun, D. Monsavais, M.E. Pavone, M. Dyson, Q. Xue, E. Attar, H. Tokunaga, E.J. Su, Role of estrogen receptor-beta in endometriosis, Semin. Reprod. Med. 30 (2012) 39–45.
[13] Q. Xue, Z. Lin, Y.H. Cheng, C.C. Huang, E. Marsh, P. Yin, M.P. Milad, E. Confino, S. Reierstad, J. Innes, S.E. Bulun, Promoter methylation regulates estrogen receptor 2 in human endometrium and endometriosis, Biol. Reprod. 77 (2007) 681–687.
[14] L.P. Stabile, S. Dacic, S.R. Land, D.E. Lenzner, R. Dhir, M. Acquafondata, R.J. Landreneau, J.R. Grandis, J.M. Siegfried, Combined analysis of estrogen receptor beta-1 and progesterone receptor expression identifies lung cancer patients with poor outcome, Clin. Canc. Res. 17 (2011) 154–164.
[15] G. Zhang, X. Liu, A.M. Farkas, A.V. Parwani, K.L. Lathrop, D. Lenzner, S.R. Land, H. Srinivas, Estrogen receptor beta functions through nongenomic mechanisms in lung cancer cells, Mol. Endocrinol. 23 (2009) 146–156.
[16] I. De Stefano, G.F. Zannoni, M.G. Prisco, A. Fagotti, L. Tortorella, G. Vizzielli, L. Mencaglia, G. Scambia, D. Gallo, Cytoplasmic expression of estrogen receptor beta (ERbeta) predicts poor clinical outcome in advanced serous ovarian cancer, Gynecol. Oncol. 122 (2011) 573–579.
[17] S.H. Yang, R. Liu, E.J. Perez, Y. Wen, S.M. Stevens Jr., T. Valencia, A.M. Brun-Zinkernagel, L. Prokai, Y. Will, J. Dykens, P. Koulen, J.W. Simpkins, Mitochondrial localization of estrogen receptor beta, Proc. Natl. Acad. Sci. U. S. A. 101 (2004) 4130–4135.
[18] S. Solakidi, A.M. Psarra, C.E. Sekeris, Differential subcellular distribution of estrogen receptor isoforms: localization of ERalpha in the nucleoli and ERbeta in the mitochondria of human osteosarcoma SaOS-2 and hepatocarcinoma HepG2 cell lines, Biochim. Biophys. Acta 1745 (2005) 382–392.
[19] J.Q. Chen, P.A. Russo, C. Cooke, I.H. Russo, J. Russo, ERbeta shifts from mitochondria to nucleus during estrogen-induced neoplastic transformation of human breast epithelial cells and is involved in estrogen-induced synthesis of mitochondrial respiratory chain proteins, Biochim. Biophys. Acta 1773 (2007) 1732–1746.
[20] H. Zhang, Y. Niu, J. Feng, H. Guo, X. Ye, H. Cui, Use of proteomic analysis of endometriosis to identify different protein expression in patients with endometriosis versus normal controls, Fertil. Steril. 86 (2006) 274–282.
[21] P.M. Keeney, J. Xie, R.A. Capaldi, J.P. Bennett Jr., Parkinson's disease brain mitochondrial complex I has oxidatively damaged subunits and is functionally impaired and misassembled, J. Neurosci.: Offic. J. Soc. Neurosci. 26 (2006) 5256–5264.
[22] H. Swalwell, D.M. Kirby, E.L. Blakely, A. Mitchell, R. Salemi, C. Sugiana, A.G. Compton, E.J. Tucker, B.X. Ke, P.J. Lamont, D.M. Turnbull, R. McFarland, R.W. Taylor, D.R. Thorburn, Respiratory chain complex I deficiency caused by mitochondrial DNA mutations, Eur. J. Hum. Genet. 19 (2011) 769–775.
[23] S.H. Kao, H.C. Huang, R.H. Hsieh, S.C. Chen, M.C. Tsai, C.R. Tzeng, Oxidative damage and mitochondrial DNA mutations with endometriosis, Ann. N. Y. Acad. Sci. 1042 (2005) 186–194.
[24] L.F. Carvalho, A.N. Samadder, A. Agarwal, L.F. Fernandes, M.S. Abrao, Oxidative stress biomarkers in patients with endometriosis: systematic review, Arch. Gynecol. Obstet. 286 (2012) 1033–1040.
[25] G. Achanta, R. Sasaki, L. Feng, J.S. Carew, W. Lu, H. Pelicano, M.J. Keating, P. Huang, Novel role of p53 in maintaining mitochondrial genetic stability through interaction with DNA Pol gamma, EMBO J. 24 (2005) 3482–3492.
[26] H. Zang, L. Sahlin, B. Masironi, A.L. Hirschberg, Effects of testosterone and estrogen treatment on the distribution of sex hormone receptors in the endometrium of postmenopausal women, Menopause 15 (2008) 233–239.
[27] L.C. Gemmell, K.E. Webster, S. Kirtley, K. Vincent, K.T. Zondervan, C.M. Becker, The management of menopause in women with a history of endometriosis: a systematic review, Hum. Reprod. Update 23 (2017) 481–500.
[28] L. Saavalainen, H. Lassus, A. But, A. Tiitinen, P. Harkki, M. Gissler, E. Pukkala, O. Heikinheimo, Risk of gynecologic cancer according to the type of endometriosis, Obstet. Gynecol. 131 (2018) 1095–1102.
[29] S.E. Bulun, Y.H. Cheng, M.E. Pavone, Q. Xue, E. Attar, E. Trukhacheva, H. Tokunaga, H. Utsunomiya, P. Yin, X. Luo, Z. Lin, G. Imir, S. Thung, E.J. Su, J.J. Kim, Estrogen receptor-beta, estrogen receptor-alpha, and progesterone resistance in endometriosis, Semin. Reprod. Med. 28 (2010) 36–43.
[30] M.T. Dyson, S.E. Bulun, Cutting SRC-1 down to size in endometriosis, Nat. Med. 18 (2012) 1016–1018.

[31] J. Fujimoto, R. Hirose, H. Sakaguchi, T. Tamaya, Expression of oestrogen receptor-alpha and -beta in ovarian endometriomata, Mol. Hum. Reprod. 5 (1999) 742–747.
[32] S.E. Bulun, D. Monsivais, T. Kakinuma, Y. Furukawa, L. Bernardi, M.E. Pavone, M. Dyson, Molecular biology of endometriosis: from aromatase to genomic abnormalities, Semin. Reprod. Med. 33 (2015) 220–224.
[33] D. Monsivais, M.T. Dyson, P. Yin, A. Navarro, J.S.T. Coon, M.E. Pavone, S.E. Bulun, Estrogen receptor beta regulates endometriotic cell survival through serum and glucocorticoid-regulated kinase activation, Fertil. Steril. 105 (2016) 1266–1273.
[34] R.C. Simmen, A.S. Kelley, Reversal of fortune: estrogen receptor-beta in endometriosis, J. Mol. Endocrinol. 57 (2016) F23–F27.
[35] C. Alvarez-Delgado, C.A. Mendoza-Rodriguez, O. Picazo, M. Cerbon, Different expression of alpha and beta mitochondrial estrogen receptors in the aging rat brain: interaction with respiratory complex V, Exp. Gerontol. 45 (2010) 580–585.
[36] Y.C. Hsieh, H.P. Yu, T. Suzuki, M.A. Choudhry, M.G. Schwacha, K.I. Bland, I.H. Chaudry, Upregulation of mitochondrial respiratory complex IV by estrogen receptor-beta is critical for inhibiting mitochondrial apoptotic signaling and restoring cardiac functions following trauma-hemorrhage, J. Mol. Cell. Cardiol. 41 (2006) 511–521.
[37] F. Guerra, I. Kurelac, A. Cormio, R. Zuntini, L.B. Amato, C. Ceccarelli, D. Santini, G. Cormio, F. Fracasso, L. Selvaggi, L. Resta, M. Attimonelli, M.N. Gadaleta, G. Gasparre, Placing mitochondrial DNA mutations within the progression model of type I endometrial carcinoma, Hum. Mol. Genet. 20 (2011) 2394–2405.
[38] S.P. Desai, S.N. Bhatia, M. Toner, D. Irimia, Mitochondrial localization and the persistent migration of epithelial cancer cells, Biophys. J. 104 (2013) 2077–2088.
[39] V. Paupe, J. Prudent, New insights into the role of mitochondrial calcium homeostasis in cell migration, Biochem. Biophys. Res. Commun. 500 (2018) 75–86.
[40] G. Scutiero, P. Iannone, G. Bernardi, G. Bonaccorsi, S. Spadaro, C.A. Volta, P. Greco, L. Nappi, Oxidative stress and endometriosis: a systematic review of the literature, Oxid. Med. Cell Longev. (2017) 7265238 2017.
[41] Z. Liu, Y. Gou, H. Zhang, H. Zuo, H. Zhang, Z. Liu, D. Yao, Estradiol improves cardiovascular function through up-regulation of SOD2 on vascular wall, Redox Biol. 3 (2014) 88–99.
[42] A. Giddabasappa, M.N. Bauler, C.M. Barrett, C.C. Coss, Z. Wu, D.D. Miller, J.T. Dalton, J.R. Eswaraka, GTx-822, an ER{beta}-selective agonist, protects retinal pigment epithelium (ARPE-19) from oxidative stress by activating MAPK and PI3-K pathways, Invest. Ophthalmol. Vis. Sci. 51 (2010) 5934–5942.
[43] C. Borras, J. Gambini, M.C. Gomez-Cabrera, J. Sastre, F.V. Pallardo, G.E. Mann, J. Vina, 17beta-oestradiol up-regulates longevity-related, antioxidant enzyme expression via the ERK1 and ERK2[MAPK]/NFkappaB cascade, Aging Cell 4 (2005) 113–118.
[44] G. Zhang, N. Yanamala, K.L. Lathrop, L. Zhang, J. Klein-Seetharaman, H. Srinivas, Ligand-independent antiapoptotic function of estrogen receptor-beta in lung cancer cells, Mol. Endocrinol. 24 (2010) 1737–1747.